Письма в ЭЧАЯ. А. 2011. Т. 8, № 9. С. 44–53

HYDROKINETIC PREDICTIONS FOR FEMTOSCOPY SCALES IN $A + A$ COLLISIONS IN THE LIGHT OF RECENT ALICE LHC RESULTS

Yu. M. Sinyukov [a,b], *Iu. A. Karpenko* [a]

[a] Bogolyubov Institute for Theoretical Physics, Kiev

[b] ExtreMe Matter Institute EMMI, GSI Helmholtz Zentrum für Schwerionenforschung, Darmstadt, Germany

A study of energy behavior of the pion spectra and interferometry scales is carried out for the top SPS, RHIC and for LHC energies within the hydrokinetic approach. The main mechanisms that lead to the paradoxical, at first sight, dependence of the interferometry scales on the energy growth, in particular, a decrease of $R_{\rm out}/R_{\rm side}$ ratio, are exposed. The hydrokinetic predictions for the HBT radii at LHC energies are compared with the recent results of the ALICE experiment.

PACS: 25.75.-q

INTRODUCTION

In anticipation of the start of the LHC experiments, there were presented many different theoretical views on the underlying physics at so large collision energies as well as numerous predictions for observables — a big collection of the predictions for heavy-ion collision was assembled in [1]. The similar took place on the eve of the RHIC experiments. At that «pre-RHIC» time, the future results on the correlation femtoscopy of particles, i.e., the topic of this entry, were expecting with great interest. One of the reasons was a hope to find the interferometry signature of the quark–gluon plasma (QGP). A very large value of the ratio of the two transverse interferometry radii, $R_{\rm out}$ to $R_{\rm side}$, was predicted as a signal of the QGP formation [2]. While the $R_{\rm side}$ radius is associated with the transverse homogeneity length [3], the $R_{\rm out}$ includes besides that also additional contributions, in particular, the one which is related to a duration of the pion emission. Since the lifetime of the systems obviously should grow with collision energy, if it is accompanied by an increase of the initial energy density and/or by a softening of the equation of state due to phase transition between hadron matter and quark–gluon plasma (QGP), the duration of pion emission should also grow with energy and so $R_{\rm out}/R_{\rm side}$ ratio could increase.

The RHIC experiments brought an unexpected result: the ratio $R_{\rm out}/R_{\rm side} \approx 1$ is similar or even smaller than at SPS. Another surprise was the absolute values of the radii. Naively it was expected that when the energy of colliding nuclei increases, the pion interferometry volume $V_{\rm int}$ — product of the interferometry radii in three orthogonal directions — will rise at the same maximal centrality for Pb + Pb and Au + Au collisions just proportionally to dN_π/dy. However, when experiments at RHIC start, an increase of the interferometry volume with energy turns out to be essentially smaller than if the proportionality law takes place. Both these unexpected results were called the RHIC HBT puzzle [4].

During a long period this puzzle was not solved in hydrodynamic/hybrid models of $A + A$ collisions which reproduce well the single-particle transverse spectra and their axial anisotropy in noncentral collisions described by the v_2 coefficients. Only a few years ago the main factors which allow one to describe simultaneously the spectra and femtoscopic scales at RHIC become clear. They are [5–10]: a relatively hard equation of state because of crossover transition (instead of the 1st order one) between quark–gluon and hadron phases and due to nonequilibrium composition of hadronic matter; presence of prethermal transverse flows and their anisotropy developed to thermalization time; an «additional portion» of the transverse flows owing to the shear viscosity effect and fluctuation of initial conditions. An account of these factors gives the possibility to describe well the pion and kaon spectra together with the femtoscopy data of RHIC within realistic freeze-out picture with a gradual decay of nonequilibrium fluid into observed particles [11].

Now, when the heavy-ion experiments at LHC already started, and the ALICE Collaboration published the first results on the femtoscopy in $A + A$ collisions at $\sqrt{s} = 2.76$ TeV [12], the main question is whether an understanding of the physics responsible for the space-time matter evolution in Au + Au collisions at RHIC can be extrapolated to the LHC energies, or some new «LHC HBT puzzle» is already apprehended just as it happened in the way from SPS to RHIC energies. In this note we describe the physical mechanisms responsible for the peculiarities of energy dependence of the interferometry radii and therefore solving the RHIC HBT puzzle, present the quantitative predictions given for LHC within hydrokinetic model earlier [13], and compare them with the recent ALICE LHC results and make the corresponding inference.

1. HYDROKINETIC APPROACH TO $A + A$ COLLISIONS

Let us briefly describe the main features of the HKM [6, 14]. It incorporates hydrodynamical expansion of the systems formed in $A + A$ collisions and their dynamical decoupling described by escape probabilities.

Initial Conditions. Our results are all related to the central rapidity slice where we use the boost-invariant Bjorken-like initial condition. We consider the proper time of thermalization of quark–gluon matter to be $\tau_0 = 1$ fm/c, at present there is no theoretical arguments permitting smaller value. The initial energy density in the transverse plane is supposed to be Glauber-like [15], i.e., is proportional to the participant nucleon density for Pb + Pb (SPS) and Au + Au (RHIC, LHC) collisions with zero impact parameter. The height of the distribution — the maximal initial energy density — $\epsilon(r = 0) = \epsilon_0$ is the fitting parameter. From analysis of pion transverse spectra we choose it for the top SPS energy to be $\epsilon_0 = 9$ GeV/fm^3 ($\langle\epsilon\rangle_0 = 6.4$ GeV/fm^3); for the top RHIC energy, $\epsilon_0 = 16.5$ GeV/fm^3 ($\langle\epsilon\rangle_0 = 11.6$ GeV/fm^3). The brackets $\langle\ldots\rangle$ correspond to mean value over the distribution associated with the Glauber transverse profile. We also demonstrate results at $\epsilon_0 = 40$ GeV/fm^3 and $\epsilon_0 = 60$ GeV/fm^3. In hydrokinetic model, $\epsilon_0 = 40$ GeV/fm^3 corresponds to multiplicity of charged particles $dN_{\rm ch}/d\eta \approx 1500$. We suppose that soon after thermalization, the matter created in $A + A$ collision at energies considered is in the quark gluon plasma (QGP) state.

At the time of thermalization, $\tau_0 = 1$ fm/c, the system already has developed collective transverse velocities [5, 7]. The initial transverse rapidity profile is supposed to be linear in radius r_T:

$$y_T = \alpha_{R_T}^{r_T}, \tag{1}$$

where α is the second fitting parameter and $R_T = \sqrt{\langle r_T^2 \rangle}$. Note that the fitting parameter α should absorb also a positive correction for underestimated resulting transverse flow since in this work we did not account in direct way for the viscosity effects [16] neither at QGP stage nor at hadronic one. In formalism of HKM [6], the viscosity effects at hadronic stage are incorporated in the mechanisms of the back reaction of particle emission on hydrodynamic evolution which we ignore in current calculations. Since the corrections to transverse flows which depend on unknown viscosity coefficients are unknown, we use fitting parameter α to describe the «additional unknown portion» of flows, caused by both factors: a developing of the prethermal flows and the viscosity effects in quark–gluon plasma. The best fits of the pion transverse spectra at SPS and RHIC are provided at $\alpha = 0.194$ ($\langle v_T \rangle = 0.178$) for SPS energies and $\alpha = 0.28$ ($\langle v_T \rangle = 0.25$) for RHIC ones. The latter value we use also for LHC energies aiming to analyze just the influence of energy density increase.

Equation of State. Following [6], we use at high temperatures the EoS [17] adjusted to the QCD lattice data with the baryonic chemical potential $\mu_B = 0$ and matched with chemically equilibrated multicomponent hadron resonance gas at $T = 175$ MeV. Such an EoS could be a good approximation for the RHIC and LHC energies; as for the SPS energies, we utilize it just to demonstrate the energy-dependent mechanism of formation of the space-time scales[1]. We suppose the chemical freeze-out for the hadron gas at $T_{\rm ch} = 165$ MeV [19]. It guarantees us the correct particle number ratios for all quasi-stable particles (here we calculate only pion observables) at least for RHIC. Below $T_{\rm ch}$, a composition of the hadron gas is changed only due to resonance decays into expanding fluid. We include 359 hadron states made of u, d, s quarks with masses up to 2.6 GeV. The EoS in this nonchemically equilibrated system depends now on particle number densities n_i of all the 359 particle species i: $p = p(\epsilon, \{n_i\})$. Since the energy densities in expanding system do not directly correlate with resonance decays, all the variables in the EoS depend on space-time points, and so an evaluation of the EoS is incorporated in the hydrodynamic code. We calculate the EoS below T_{ch} in the Boltzmann approximation of ideal multicomponent hadron gas.

Evolution. At the temperatures higher than $T_{\rm ch}$, the hydrodynamic evolution is related to the quark–gluon and hadron phases which are in chemical equilibrium with zero baryonic chemical potential. The evolution is described by the conservation law for the energy-momentum tensor of perfect fluid:

$$\partial_\nu T^{\mu\nu}(x) = 0. \tag{2}$$

At $T < T_{\rm ch} = 165$ MeV, the system evolves as nonchemically equilibrated hadronic gas. The concept of the chemical freeze-out implies that afterwards only elastic collisions and resonance decays take place because of relatively small densities allied with a fast rate of expansion at the last stage. Thus, in addition to (2), the equations accounting for the particle number conservation and resonance decays are added. If one neglects the thermal motion of heavy resonances, the equations for particle densities $n_i(x)$ take the form:

$$\partial_\mu (n_i(x) u^\mu(x)) = -\Gamma_i n_i(x) + \sum_j b_{ij} \Gamma_j n_j(x), \tag{3}$$

[1] A good description of the spectra and HBT radii at the SPS energies with realistic EoS within hydrokinetic model is presented in [18].

where $b_{ij} = B_{ij}N_{ij}$ denote the average number of ith particles coming from arbitrary decay of jth resonance; $B_{ij} = \Gamma_{ij}/\Gamma_{j,\mathrm{tot}}$ is branching ratio; N_{ij} is a number of ith particles produced in $j \to i$ decay channel. We also can account for recombination in the processes of resonance decays into expanding medium just by utilizing the effective decay width $\Gamma_{i,\mathrm{eff}} = \gamma\Gamma_i$. We use $\gamma = 0.75$ supposing thus that near 30% of resonances are recombining during the evolution. All the equations (2) and 359 equations (3) are solved simultaneously with calculation of the EoS, $p(x) = p(\epsilon(x), \{n_i(x)\})$, at each point x.

System's Decoupling and Spectra Formation. During the matter evolution, in fact, at $T \leqslant T_{\mathrm{ch}}$, hadrons continuously leave the system. Such a process is described by means of the emission function $S(x,p)$ which is expressed for pions through the *gain* term, $G_\pi(x,p)$, in Boltzmann equations and the escape probabilities $\mathcal{P}_\pi(x,p) = \exp\left(-\int\limits_t^\infty ds\, R_{\pi+h}(s, \mathbf{r} + {}+{}^{\mathbf{p}}_{p^0}(s-t), p)\right)$: $S_\pi(x,p) = G_\pi(x,p)\mathcal{P}_\pi(x,p)$ [6, 14]. For pion emission in relaxation time approximation $G_\pi \approx f_\pi R_{\pi+h} + G_{H\to\pi}$, where $f_\pi(x,p)$ is the pion Bose–Einstein phase-space distribution, $R_{\pi+h}(x,p)$ is the total collision rate of the pion, carrying momentum p, with all the hadrons h in the system in a vicinity of point x; the term $G_{H\to\pi}$ describes an inflow of the pions into phase-space point (x,p) due to the resonance decays. It is calculated according to the kinematics of decays with simplification that the spectral function of the resonance H is $\delta(p^2 - \langle m_H\rangle^2)$. The cross sections in the hadronic gas, that determine via the collision rate $R_{\pi+h}$ the escape probabilities $\mathcal{P}(x,p)$ and emission function $S(x,p)$, are calculated in accordance with the UrQMD method [20]. The spectra and correlation functions are found from the emission function S in the standard way (see, e.g., [14]).

2. RESULTS AND CONCLUSIONS

The pion emission function per unit (central) rapidity, integrated over azimuthal angular and transverse momenta, is presented in Fig. 1 for the top SPS, RHIC, and LHC energies as a function of transverse radius r and proper time τ. The two fitting parameters and $\langle v_T\rangle$ are fixed as discussed above, ϵ_0 is also marked in figures. The pion transverse momentum spectrum, its slope as well as the absolute value, and the interferometry radii, including R_{out} to R_{side} ratio, are in good agreement with the experimental data for both the top SPS and RHIC energies.

As one can see, particle emission lasts a total lifetime of the fireballs; in the cental part, $\mathbf{r} \approx 0$, the duration is half of the lifetime. Nevertheless, according to the results [6, 21], the Landau/Cooper–Frye presentation of sudden freeze-out could be applied in a generalized form accounting for momentum dependence of the freeze-out hypersurface $\sigma_p(x)$; now $\sigma_p(x)$ corresponds to the *maximum of emission function* $S(t_\sigma(\mathbf{r},p), \mathbf{r}, p)$ at fixed momentum $\mathbf{p}$ in an appropriate region of $\mathbf{r}$. This finding allows one to keep in mind the known results based on the Cooper–Frye formalism, applying them to a surface of the maximal emission for given p. Then the typical features of the energy dependence can be understood as follows. The inverse of the spectra slopes, T_{eff}, grows with energy, since, as one sees from the emission functions, the duration of expansion increases with initial energy density and, therefore, the pressure gradient driven fluid elements get more transverse collective velocities v_T when reach a decoupling energy densities. Therefore the blue shift of the spectra becomes stronger. A rise

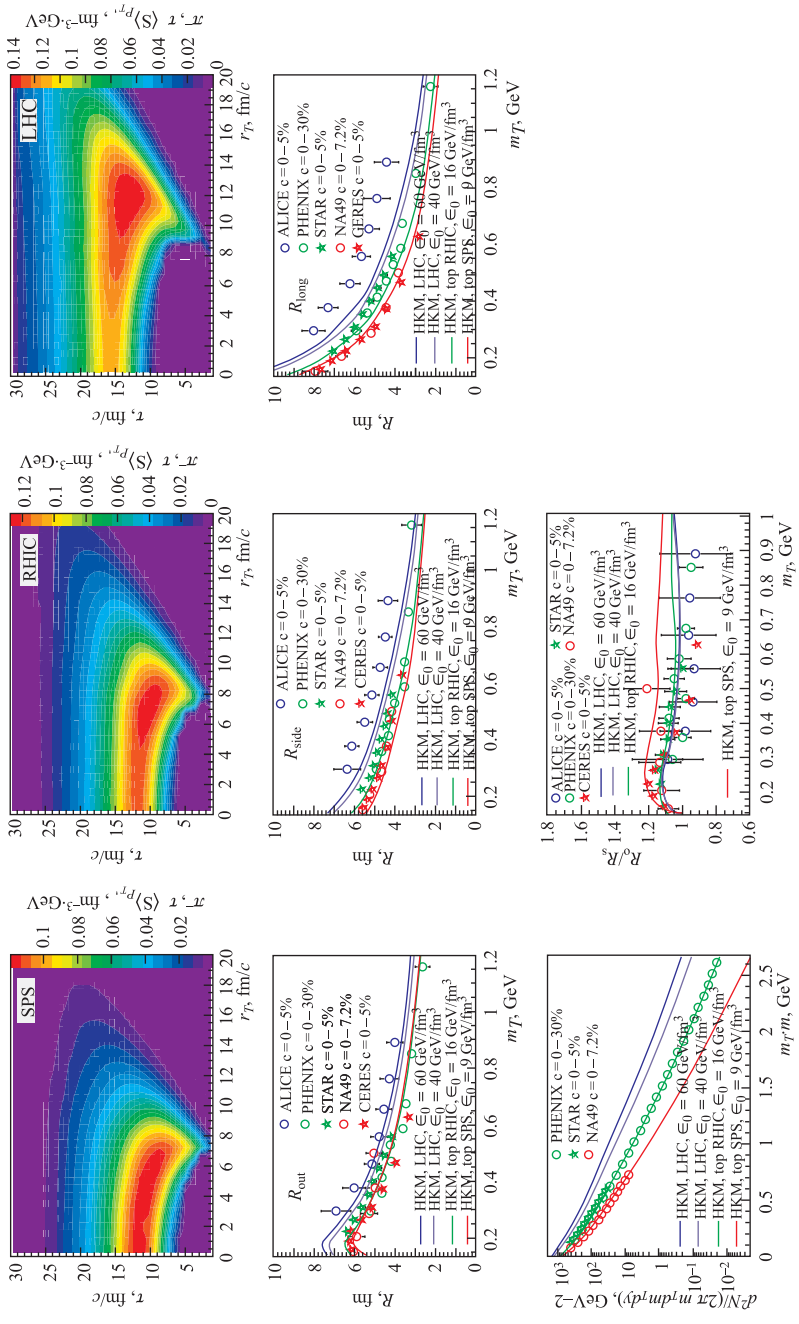

Fig. 1. The p_T-integrated emission functions of negative pions for the top SPS, RHIC, and LHC energies (top); the interferometry radii (middle), $R_{\rm out}/R_{\rm side}$ ratio and transverse momentum spectra (bottom) of negative pions at different energy densities, all calculated in HKM model. The experimental data are taken from CERES [27] and NA49 Collaborations [28, 29] (SPS CERN), STAR [30, 31] and PHENIX [32, 33] Collaborations (RHIC BNL) and ALICE Collaboration (LHC, CERN) [12]

of the transverse collective flow with energy leads to some compensation of an increase of $R_{\rm side}$: qualitatively the homogeneity length at decoupling stage is $R_{\rm side} = R_{\rm geom}/\sqrt{1+\langle v_T^2\rangle m_T/2T}$ (see, e.g., [22]). So, despite a significant increase of the transverse emission region, $R_{\rm geom}$, seen in Fig. 1, a magnification of collective flow partially compensates this. It leads to only a moderate increase of the $R_{\rm side}$ with energy. Since the temperatures in the regions of the maximal emission decrease very slowly when initial energy density grows (e.g., the temperatures for SPS, RHIC, and LHC are correspondingly 0.105, 0.103, and 0.95 MeV for $p_T = 0.3$ GeV/c), the $R_{\rm long} \sim \tau\sqrt{T/m_T}$ [23] grows proportionally to an increase of the proper time associated with the hypersurface $\sigma_{p_T}(x)$ of *maximal* emission. As we see from Fig. 1 this time grows quite moderate with the collision energy.

A nontrivial result concerns the energy behavior of the $R_{\rm out}/R_{\rm side}$ ratio. It slowly drops when energy grows and apparently is saturated at fairly high energies at the value close to unity (Fig. 1). To clarify the physical reason of it, let us make a simple half-quantitative analysis. As one can see in Fig. 1, the hypersurface of the maximal emission can be approximated as consisting of two parts: the «volume» emission (V) at $\tau \approx$ const and «surface» emission (S). A similar picture within the Cooper–Frye prescription, which generalizes the blast-wave model [24] by means of including of the surface emission, has been considered in [25]. If the hypersurface of maximal emission $\tilde{\tau}(r)$ is double-valued function, as in our case, then at some transverse momentum p_T the transverse spectra and HBT radii will be formed mostly by the two contributions from the different regions with the homogeneity lengths $\lambda_{i,V} = \sqrt{\langle(\Delta r_i)^2\rangle}$ ($i =$ side, out) at the V-hypersurface and with the homogeneity lengths $\lambda_{i,S}$ at the S-hypersurface. Similar to [22], one can apply at $m_T/T \gg 1$ the saddle point method when calculating the single and two particle spectra using the boost-invariant measures $\mu_V = d\sigma_\mu^V p^\mu = \tilde{\tau}(r) r\, dr\, d\phi\, d\eta(m_T \cosh(\eta - y) - p_T \dfrac{d\tilde{\tau}(r)}{dr}\cos(\phi-\alpha))$ and $\mu_S = d\sigma_\mu^S p^\mu = \tilde{r}(\tau)\tau\, d\tau\, d\phi\, d\eta(-m_T\cosh(\eta - y)\dfrac{d\tilde{r}(\tau)}{d\tau} + p_T\cos(\phi-\alpha))$ for V- and S- parts of freeze-out hypersurface correspondingly (here η and y are space-time and particle pair rapidities, the similar correspondence is for angles ϕ and α, also note that $p_T/m_T > d\tilde{r}(\tau)/d\tau$ [6, 21]). Then one can write, ignoring for simplicity the interference (cross-terms) between the surface and volume contributions,

$$R_{\rm side}^2 = c_V^2\lambda_{{\rm side},V}^2 + c_S^2\lambda_{{\rm side},S}^2, \tag{4}$$

$$R_{\rm out}^2 = c_V^2\lambda_{{\rm out},V}^2 + c_S^2\lambda_{{\rm out},S}^2(1 - \frac{d\tilde{r}}{d\tau})^2, \tag{5}$$

where the coefficients $c_V^2 + c_S^2 \leqslant 1$, and we take into account that at $p^0/T \gg 1$ for pions $\beta_{\rm out} = p_{\rm out}/p^0 \approx 1$. All homogeneity lengths depend on mean transverse momentum of the pion pairs p_T. The slope $d\tilde{r}/d\tau$ in the region of homogeneity expresses the strength of $r - \tau$ correlations between the space and time points of particle emission at the S-hypersurface $\tilde{r}(\tau)$. The picture of emission in Fig. 1 shows that when the energy grows, the correlations between the time and radial points of the emission become positive, $d\tilde{r}/d\tau > 0$, and they increase with energy density. The positivity is caused by the initial radial flows [5] $u^r(\tau_0)$, which are developed at the prethermal stage, and the strengthening of the $r - \tau$ correlations happens because the noncentral ith fluid elements, which produce after their expansion the surface emission, need more time $\tau_i(\epsilon_0)$ to reach the decoupling density if they initially have higher energy density ϵ_0. (Let us characterize this effect by the parameter

$\kappa = d\tau_i(\epsilon_0)/d\epsilon_0 > 0$). Then the fluid elements before their decays run up to larger radial freeze-out position r_i: if a is the average Lorentz-invariant acceleration of those fluid elements during the system expansion, then roughly for ith fluid elements which decay at time τ_i we have at $a\tau_i \gg 1$: $r_i(\tau_i) \approx r_i(\tau_0) + \tau_i + (u_i^r(\tau_0) - 1)/a$. Then the level of $r{-}\tau$ correlations within the homogeneous freeze-out «surface» region, which is formed by the expanding matter that initially at τ_0 occupies the region between the transversal radii $r_1(\tau_0)$ and $r_2(\tau_0) > r_1(\tau_0)$, is

$$\frac{d\tilde{r}}{d\tau} \approx \frac{r_1(\tau_1) - r_2(\tau_2)}{\tau_1 - \tau_2} \approx 1 - \frac{R}{\epsilon_0 \kappa}, \tag{6}$$

and, therefore, the strength of $r{-}\tau$ correlations grows with energy: $d\tilde{\tau}/dr \to 1$. Note that here we account for $\tau_2 - \tau_1 \approx \kappa(\epsilon_0(r_2(\tau_0)) - \epsilon_0(r_1(\tau_0)))$ and that $d\epsilon_0(r)/dr \approx -\epsilon_0/R$, where $\epsilon_0 \equiv \epsilon_0(r = 0)$ and R is radius of nucleus. As a result, the second S term in Eq. (5) tends to zero at large ϵ_0, reducing, therefore, the $R_{\rm out}/R_{\rm side}$ ratio. In particular, if $\lambda^2_{{\rm side},V} \gg \lambda^2_{{\rm side},S}$, then, accounting for a similarity of the volume emission in our approximation and in the blast wave model, where as known $\lambda_{{\rm side},V} \approx \lambda_{{\rm out},V}$, one can get: $R_{\rm out}/R_{\rm side} \approx 1 + {\rm const}\, R/\epsilon_0\kappa \to 1$ at $\epsilon_0 \to \infty$. It is worthy of note that also measure μ_S tends to zero when $d\tilde{\tau}/dr \to 1$ that again reduces the surface contribution to *side*- and *out*-radii at large p_T.

The presented qualitative analysis demonstrates the main mechanisms responsible for the nontrivial behavior of $R_{\rm out}$ to $R_{\rm side}$ ratio exposed in HKM calculations, see Fig. 1 (bottom). The very recent first LHC data for Pb+Pb collisions presented by the ALICE Collaboration [12] conform, in fact, the discussed above physical picture of space-time evolution responsible for formation of the HBT radii and $R_{\rm out}$ to $R_{\rm side}$ ratio, see Fig. 1. The transverse femtoscopy scales, predicted for the charged multiplicity $dN_{\rm ch}/d\eta = 1500$ in HKM at the initial energy density $\epsilon_0 = 40$ GeV/fm^3, are quite close to the experimental data associated with $dN_{\rm ch}/d\eta \approx 1600$ at the collision energy $\sqrt{s} = 2.76$ TeV. As for the longitudinal HBT radius, $R_{\rm long}$, it is underestimated in HKM by around 20%. As a result, HKM gives smaller interferometry volume than is observed at LHC. The reason could be that HKM describes a gradual decay of the system which evolves hydrodynamically until fairly large times. It is known [26] that at the isentropic and chemically frozen hydrodynamic evolution, the interferometry volume increases quite moderate with initial energy density growth in collisions of the same/similar nucleus. The RHIC results support such a theoretical view (see solid line in Fig. 2), while the ALICE Collaboration observes a significant increase of the interferometry volume at LHC. One should change, thus, the global fit of $V_{\rm int}(dN/d\eta)$ for $A + A$ collisions for steeper slope (upper dashed line). However, no one linear fit cannot be extrapolated to $V_{\rm int}(dN/d\eta)$-dependence discovered by the ALICE Collaboration in $p + p$ collisions [34] (bottom dashed line in Fig. 2). Could one call these two observed peculiarities as the «LHC HBT puzzle»? In our opinion, at least qualitatively, it is not puzzling. An essential growth of the interferometry volume in Pb + Pb collisons at the first LHC energy can be conditioned by an increase of the duration of the last very nonequilibrium stage of the matter evolution which cannot be considered on the hydrodynamic basis, and one should use hadronic cascade models like UrQMD. At such late stage, the results obtained in [26] for isentropic and chemically frouzen evolution are violated. As for the different linear $V_{\rm int}(dN/d\eta)$ dependence in $A + A$ and $p + p$ collisions, the interferometry volume depends not only on multiplicity but also on intial size of colliding systems [26]. Therefore, qualitatively, we see no puzzle in the newest HBT results obtained at LHC in Pb + Pb and $p + p$ collisions, but the final concusion can be done only after detailed quantitative analysis.

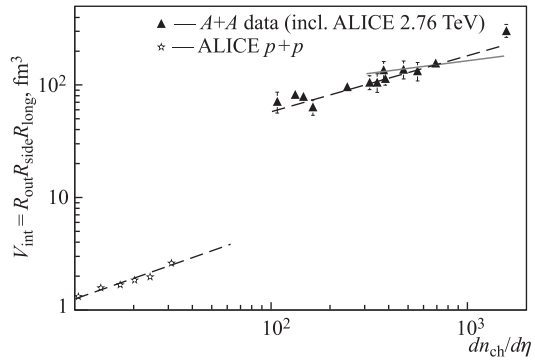

Fig. 2. Illustration of multiplicity dependence of the pion inteferometry volume on charged-particle multiplicity for central heavy-ion collisions at AGS, SPS, RHIC, and LHC energies and comparison with the results in $p + p$ collisions (bottom, left). All the HBT radii are taken at the pion transverse momentum $p_T = 0.3$ GeV. For $A + A$ collision the data are taken from Fig. 4 of [12] (see all details there); for $p + p$ collisions the points for $p_T = 0.3$ GeV are interpolated from the results of [34]. The solid line corresponds to a linear fit of $V_{\rm int}(dN_{\rm ch}/d\eta)$-dependence only for the top SPS and the RHIC energies; upper dashed line is a fit for all the $A + A$ energies including the newest LHC point at $\sqrt{s} = 2.76$ TeV; the bottom dashed line is a linear fit for ALICE LHC results for $p + p$ collisions with energies 0.9 and 2.76 TeV

Summary. We conclude that energy behavior of the pion interferometry scales can be understood at the same hydrokinetic basis as for the SPS and RHIC energies supplemented by hadronic cascade model at the latest stage of the evolution. In this approach, the EoS accounts for a crossover transition between quark–gluon and hadron matters at high collision energies and nonequilibrated expansion of the hadron-resonance gas at the later stage.

The HKM alows one to treat correctly the process of particle emission from expanding fireball, that is not sudden and lasts about the system's lifetime. Also it takes into account the prethermal formation of transverse flows. Then, the main mechanisms that lead to the paradoxical behavior of the interferometry scales find a natural explanation. In particular, a slow decrease and apparent saturation of $R_{\rm out}/R_{\rm side}$ ratio around unity at high energy happens due to a strengthening of positive correlations between space and time positions of pions emitted at the radial periphery of the system. Such an effect is a consequence of the two factors accompanying an increase of collision energy: a developing of the prethermal collective transverse flows and an increase of initial energy density in the fireball. The predictions of the HKM for LHC energies are quite close to the first experimental data in Pb + Pb collisions at LHC.

Acknowledgements. Yu. S. gives thanks to P. Braun-Munzinger for support of this study within EMMI/GSI organizations as well as for fruitful and very stimulating discussions. The researches were carried out in part within the scope of the EUREA: European UltraRelativistic Energies Agreement (European Research Group GDRE: Heavy ions at ultrarelativistic energies) and is supported by the State Fund for Fundamental Researches of Ukraine (Agreement of 2011) and National Academy of Sciences of Ukraine (Agreement of 2011).

REFERENCES

1. *Armesto N. et al.* // J. Phys. 2008. V. 35. P. 054001.
2. *Bertsch G.* // Phys. Rev. C. 1989. V. 40. P. 1830;
   Rischke D. H., Gyulassy M. // Nucl. Phys. A. 1996. V. 608. P. 479.
3. *Sinyukov Yu. M.* // Nucl. Phys. A. 1994. V. 566. P. 589c;
   Sinyukov Yu. M. // Hot Hadronic Matter: Theory and Experiment / Eds.: J. Letessier, H. H. Gutbrod, and J. Rafelski. N. Y.: Plenum, 1995. P. 309.
4. *Heinz U.* // Nucl. Phys. A. 2003. V. 721. P. 30;
   Pratt S. // Nucl. Phys. A. 2003. V. 715. P. 389c;
   Soff S. et al. // Nucl. Phys. A. 2003. V. 715. P. 801c.
5. *Sinyukov Yu. M.* // Acta Phys. Polon. B. 2006. V. 37. P. 4333;
   Gyulassy M. et al. // Braz. J. Phys. 2007. V. 37. P. 1031.
6. *Akkelin S. V. et al.* // Phys. Rev. C. 2008. V. 78. P. 034906.
7. *Sinyukov Yu. M., Karpenko Iu. A., Nazarenko A. V.* // J. Phys. G: Nucl. Part. Phys. 2008. V. 35. P. 104071.
8. *Broniowski W. et al.* // Phys. Rev. C. 2009. V. 80. P. 034902.
9. *Sinyukov Yu. M., Nazarenko A. V., Karpenko Iu. A.* // Act. Phys. Pol. B. 2009. V. 40. P. 1109.
10. *Pratt S.* // Nucl. Phys. A. 2009. V. 830. P. 51c–57c.
11. *Karpenko Iu. A., Sinyukov Yu. M.* // Phys. Rev. C. 2010. V. 81. P. 054903.
12. *Aamodt K. et al. (ALICE Collab.)* // Phys. Lett. B. 2011. V. 696. P. 328.
13. *Karpenko Iu. A., Sinyukov Yu. M.* // Phys. Lett. B. 2010. V. 688. P. 50.
14. *Sinyukov Yu. M., Akkelin S. V., Hama Y.* // Phys. Rev. Lett. 2002. V. 89. P. 052301.
15. *Kolb P. F., Sollfrank J., Heinz U.* // Phys. Lett. B. 1999. V. 459. P. 667; Phys. Rev. C. 2000. V. 62. P. 054909.
16. *Teaney D.* // Phys. Rev. C. 2003. V. 68. P. 034913.
17. *Laine M., Schröder Y.* // Phys. Rev. D. 2006. V. 73. P. 085009.
18. *Karpenko Iu. A. et al.* arXiv 2010 [nucl-th]. N.1012.2312.
19. *Becattini F., Manninen J.* // J. Phys. G: Nucl. Part. Phys. 2008. V. 35. P. 104013;
    Andronic A., Braun-Munzinger P. , Stachel J. arXiv: 2008:0812.1186; arXiv: 2009:0901.2909.
20. *Bleicher M. et al.* // J. Phys. G: Nucl. Part. Phys. 1999. V. 25. P. 1859.
21. *Sinyukov Yu. M., Akkelin S. V., Karpenko Iu. A.* // Acta Phys. Polon. B. 2009. V. 40. P. 1025.
22. *Akkelin S. V., Sinyukov Yu. M.* // Phys. Lett. B. 1995. V. 356. P. 525;
    Akkelin S. V., Sinyukov Yu. M. // Z. Phys. C. 1996. V. 72. P. 501.
23. *Makhlin A. N., Sinyukov Yu. M.* // Z. Phys. C. 1988. V. 39. P. 69.
24. *Schnedermann E., Sollfank J., Heinz U.* // Phys. Rev. C. 1993. V. 48. P. 2462.
25. *Borysova M. S. et al.* // Phys. Rev. C. 2006. V. 73. P. 024903.
26. *Akkelin S. V., Sinyukov Yu. M.* // Phys. Rev. C. 2004. V. 70. P. 064901; Phys. Rev. C. 2006. V. 73. P. 034908.
27. *Antończyk Dariusz* // Acta Phys. Polon. B. 2009. V. 40. P. 1137.
28. *Afanasiev S. V. et al. (NA49 Collab.)* // Phys. Rev. C. 2002. V. 66. P. 054902.
29. *Alt C. et al. (NA49 Collab.)* // Phys. Rev. C. 2008. V. 77. P. 064908.

30. *Adams J. et al. (STAR Collab.)* // Phys. Rev. Lett. 2004. V. 92. P. 112301.
31. *Adams J. et al. (STAR Collab.)* // Phys. Rev. C. 2004. V. 71. P. 044906.
32. *Adler S. S. et al. (PHENIX Collab.)* // Ibid. V. 69. P. 034909.
33. *Adler S. S. et al. (PHENIX Collab.)* // Phys. Rev. Lett. 2004. V. 93. P. 152302.
34. *The ALICE Collab.* arXiv: [hep-ex] 2011:1101.3665.